Received: 21 April 2020 | Revised: 13 July 2020 | Accepted: 4 August 2020

DOI: 10.1111/jocd.13690

JCD Journal of Cosmetic Dermatology

WILEY

ORIGINAL CONTRIBUTION

An evaluation of electrocoagulation and thermal diffusion following radiofrequency microneedling using an in vivo porcine skin model

Shaun Wootten BSE[1] | Zosia E. Zawacki VMD[2] | Lawrence Rheins PhD[1] | Carol Meschter DVM, PhD, DACVP[2] | Zoe Diana Draelos MD[3]

[1]Department of Research and Development, Aesthetics Biomedical Inc., Phoenix, AZ, USA

[2]Department of Research Services, Comparative Biosciences Inc., Sunnyvale, CA, USA

[3]Dermatology Consulting Services, PLLC, High Point, NC, USA

Correspondence
Shaun Wootten, Director of Research and Development, Aesthetics Biomedical, Inc, 4602 N 16th St. Suite 300, Phoenix, AZ 85016, USA.
Email: ShaunW@aestheticsbiomed.com

Funding information
This study was funded by Aesthetics Biomedical Inc, Phoenix, Arizona, USA.

Abstract

Background: Few studies exist that examined the role of radiofrequency microneedling (RFMN) in skin electrocoagulation. This research utilized a porcine model to understand bipolar dermal delivery from an RFMN device.

Aims: The objective of this study was to elucidate and compare the dermal thermal effects of a RFMN device producing 1 and 2 MHz signal amplitudes, with respective voltage and current gradients, utilizing noninsulated and insulated needles by examining the histologic effects on porcine skin.

Methods: Two separate animal studies were conducted to evaluate the electrocoagulation and thermal diffusion effects using the RFMN device. The electrocoagulation effects were assessed histologically using hematoxylin and eosin (H&E) staining, and heating effects were assessed through thermal imaging.

Results: Histology results of the thermal injury induced by insulated needles demonstrated that 2 MHz resulted in a narrow and concentrated coagulation zone as compared to 1 MHz. Further, the 1 MHz insulated needle resulted in ovular shaped tissue coagulation as compared to 2 MHz tissue coagulation that was columnar. Finally, full thermal diffusion occurs seconds after the set RF conduction time.

Conclusion: The findings showed that 1 MHz insulated needle produces larger coagulations with an increase in power level, the 1 MHz noninsulated array was comparable to the 2 MHz insulated array with similar histologic features, and heat dissipates seconds after the set conduction time.

KEYWORDS

dermal heating, electrocoagulation, microneedling, radiofrequency, skin tightening

1 | INTRODUCTION

Radiofrequency (RF) devices and lasers are currently used to treat facial photoaging and scarring.[1-4] When treating photoaging and scarring, it is important to avoid or minimize epidermal thermal damage to mitigate patient downtime and to avoid postinflammatory hyperpigmentation (PIH) or hypopigmentation from occurring.[5] Radiofrequency has the capability to ignore epidermal melanin, while lasers that use an optical energy output operate on the principle of selective photothermolysis.[3] Radiofrequency shows to be the modality of choice over ablative lasers when avoiding significant patient downtime and epidermal damage.

Radiofrequency devices differ from lasers in that they employ an oscillating electrical current, whereas lasers utilize an electrical current to excite electrons within a gas, crystal, or glass to emit light. RF devices may deliver mono-polar or bipolar energy. Mono-polar RF involves two poles, where one pole is a negative ground plate and the other pole is the applicator plate that establishes the radiofrequency. Mono-polar RF is used when greater depth of penetration and higher volumetric heating are desired, which are important for body contouring and fat dissolution. Bipolar RF, on the other hand, involves two or more active electrodes where one electrode is positive and the other is negative.[6,7] The microneedles are the electrodes for radiofrequency microneedling (RFMN). Bipolar RF has an advantage over mono-polar RF because the thermal injury can be confined to a specific skin layer compared to mono-polar RF where less control exists. Bipolar radiofrequency is selected when precision and sparing of the epidermal and subcutaneous layers are desired. This is necessary when treating facial photodamage.

Commercial RFMN devices differ from one another by placing the needles in various geometric configurations, varying the number of needles in the array, insulating the needles with a variety of materials to control RF diffusion, using uninsulated needles to give a noninsulated RF needle effect, angling the needles, and controlling the RF energy to target various tissue depths.

The current study histologically and thermally examined the RF propagation of insulated and noninsulated needles in a porcine model with a set depth, set RF conduction time, selected power level, and at 1 and 2 MHz frequencies.

2 | METHODS

Two study protocols were approved by the Institutional Animal Care and Use Committee (IACUC) and were carried out in accordance with the approved guidelines.

2.1 | Study 1

Study 1 utilized two female Yorkshire pigs, weighing 46-47 kg, that were acclimated for 1 week. Yorkshire pigs were selected due to their size because of surface area needs for RFMN application sites. The animals were acquired through an approved vendor and acclimated under standard housing provisions for 5 days prior to start of study. Clinical observations, including all signs of clinical abnormalities, were recorded once daily during acclimation to ensure health of the animal for the study. RFMN treatment (Vivace; SHENB Co., Ltd.; Figure 1) was performed on the pig dorsum with the 6 × 6 square needle array that penetrated the dermis. Animals were anesthetized with an intramuscular injection of tiletamine and zolazepam and maintained on isoflurane oxygen. The animals were then positioned

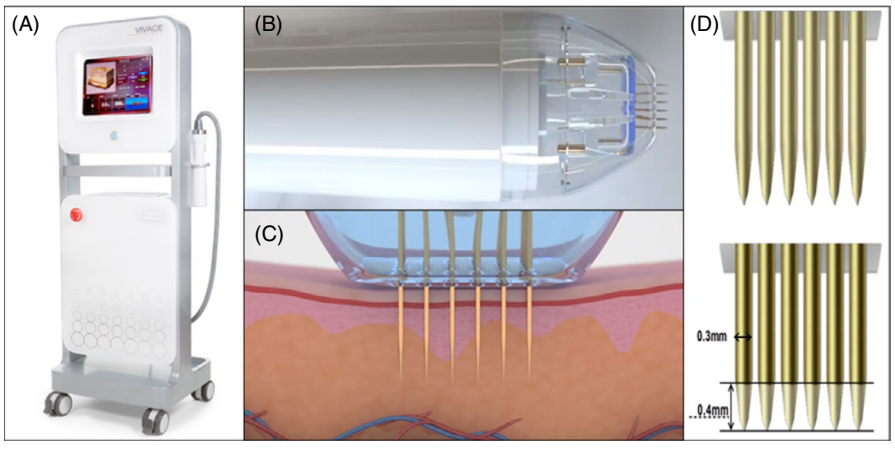

FIGURE 1 RFMN Device. A, Device design. B, Handpiece side view with attached microneedle cartridge. C, Microneedle cartridge with protruding needles into dermal layer. D, Illustration of noninsulated microneedles (top) and insulated microneedles (bottom)

TABLE 1 RFMN system voltage (V) and current (mA) table for power level

Power level	1	2	3	4	5	6	7	8	9	10
1 MHz (V)	4	13	33	56	60	64	86	96	110	134
1 MHz (mA)	4	8	18	27	29	33	40	45	51	62
2 MHz (V)	1.1	4.4	6.5	16	34	42	54	72	85	99
2 MHz (mA)	1.5	2.6	3.6	8	17	22	29	38	46	55

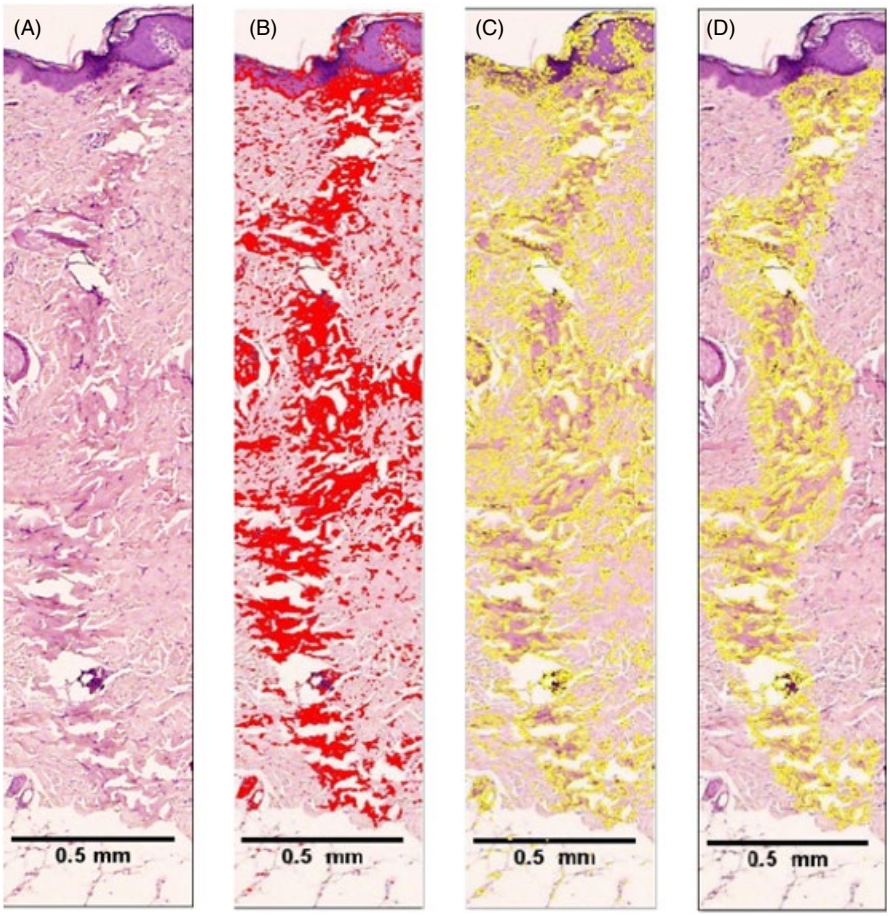

FIGURE 2 Image processing technique for area analysis of nonuniform shapes using ImageJ. A, H&E image of RFMN event. B, Threshold color to show electrocoagulation. C, Raw selection of threshold color. D, Electrocoagulation with the reduction of noise for area analysis

in lateral recumbency where the right dorsal side was treated. The skin of the thoracic and dorsal regions was shaved and prepped. Grids were marked with indelible ink to denote device application sites. Each application site represented a 36-microneedle array with set RF parameters: insulated or noninsulated microneedle, power level, depth, RF conduction time, and RF frequency of 1 or 2 MHz. The voltage and current values for each power level are listed in Table 1. Each application site was spaced 1-cm apart to eliminate RF and thermal effects from adjacent treatment areas. A total of 56 applications were performed on each animal.

One hour after each treatment, a 3-5 mm punch biopsy was taken of each single needle site. The needle array is a 10 × 10 mm with microneedles being 0.3 mm in diameter and needle to needle spacing being 1.67 mm. Untreated control biopsies were also taken. Treated and control skin biopsies were fixed in 10% neutral buffered formalin (NBF), embedded in paraffin, and then stained with hematoxylin and eosin (H&E). Processed treated and

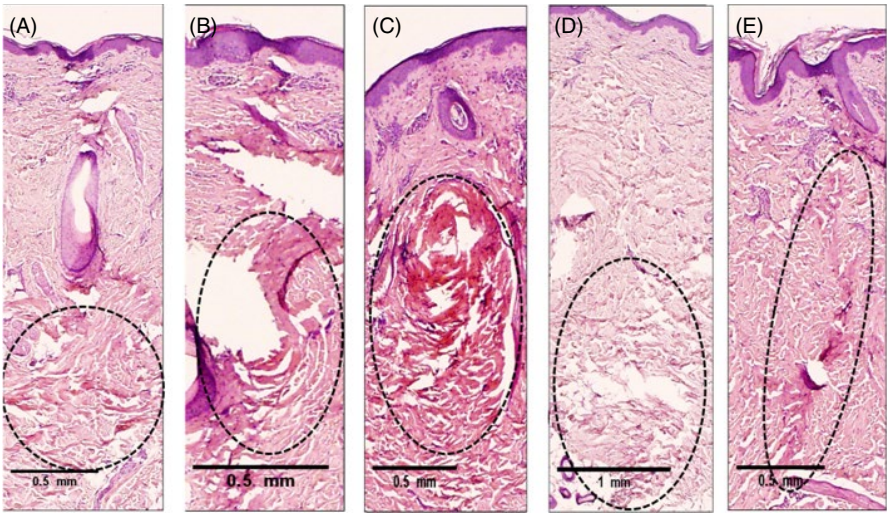

FIGURE 3 Tissue reactions after 1 MHz bipolar radiofrequency (RF) treatment using insulated microneedle electrodes on in vivo porcine skin. Porcine skin shows thermal injury in the dermis induced by radiofrequency with set parameters—1 MHz invasive bipolar RF, power level 4(A), 5(B), 6(C), 7(D), 8(E), conduction time of 600 ms, penetration depth of 2 mm using a electrosurgical microneedling unit

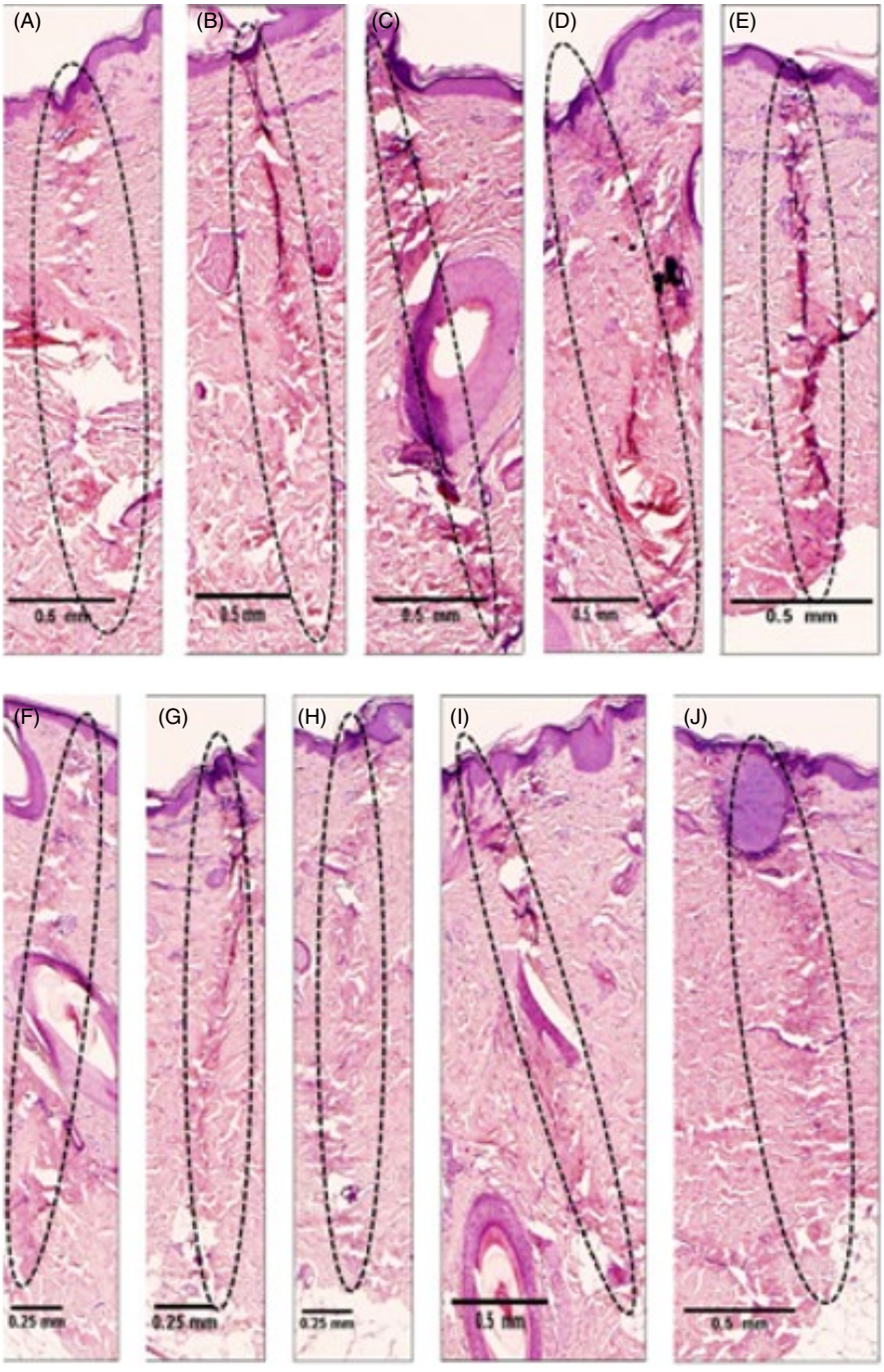

FIGURE 4 Tissue reactions after 2 MHz bipolar RF treatment using insulated microneedle electrodes (A-E) and 1 MHz invasive bipolar RF using noninsulated microneedle electrodes (F-J) on in vivo porcine skin. Porcine skin shows thermal injury similarities when using 2 MHz insulated microneedle electrode RF compared to 1 MHz noninsulated microneedle electrode RF in the dermis with set parameters—2 MHz (A-E) and 1 MHz (F-J) invasive bipolar RF, power level 4(A, F), 5(B, G), 6(C, H), 7(D, I), 8(E, J), conduction time of 600 ms, penetration depth of 2 mm using a electrosurgical microneedling unit

untreated H&E specimens were evaluated using the ImageJ (NIH, 2018) digital analysis image processing tool comparing the areas of coagulation.

The area of coagulation was evaluated after bipolar RF using an insulated and noninsulated microneedle at 1 and 2 MHz. The electrocoagulation images (Figure 2A) were evaluated using *Hue*, *Saturation*, *Brightness* (HSB) color space with a red threshold color and the ImageJ default thresholding method (Figure 2B). Once isolated, the threshold image was selected, and an area analysis was then used to obtain the initial area value (Figure 2C). The selection tool was then used to isolate the coagulation region further to obtain a quantitative area measurement (Figure 2D).

2.2 | Study 2

A thermal imaging study was also undertaken on three Yucatan minipigs, weighing approximately 20 kg. Yucatan minipigs were selected for their size for the study due to the study not needing large amounts of surface area like Study 1. The animals were acquired through an approved vendor and acclimated under standard housing provisions for 5 days prior to start of study. Clinical observations, including all signs of clinical abnormalities, were recorded once daily during acclimation to ensure health of the animal for the study. Animals were anesthetized with an intramuscular injection of tiletamine and zolazepam and maintained on isoflurane oxygen. The

TABLE 2 Area analysis of electrocoagulation. A, 1 MHz noninsulated microneedle coagulation area B, 1 MHz insulated microneedle coagulation area (C) 2 MHz insulated microneedle coagulation area; 2 MHz noninsulated microneedle coagulation area is not shown in the table due to coagulations not apparent when analyzing the histology

Area analysis of electrocoagulation				
Level 4	Level 5	Level 6	Level 7	Level 8
(A) 1 MHz noninsulated area (mm^2)				
0.149	0.109	0.304	0.206	0.451
(B) 1 MHz insulated area (mm^2)				
0.168	0.233	0.470	0.660	0.341
(c) 2 MHz insulated area (mm^2)				
0.304	0.194	0.287	0.291	0.266

animals were placed in sternal recumbency. A 10 × 10 cm dorsal skin flap was created and elevated toward the midline. The animal will be positioned in lateral recumbency such that the skin flap is retracted parallel to the table so that a thermal imaging system (FLIR A325 sc) can be positioned underneath the dermal surface of the flap to record the thermal diffusion effects after RFMN treatment. Additional flaps were then made, as needed, along the dorsum, when the prior dorsal skin flap could not be used due to the area of skin already being treated. The skin flap thickness was measured each time by caliper at the proximal, medial, and distal flap to ensure the proceeding skin flaps were similar in size. The thicknesses were recorded and the depth parameters optimized. The needle depth was 1 mm from the bottom of the skin flap. Needle depth would be adjusted due to skin flap thickness measurement. The following formula was used: Skin Flap Thickness (mm) − 1 mm = Needle Depth. Cautery was used to achieve hemostasis along the skin flap margins. Cautery was not used inside the margins where the RFMN was applied. A RFMN treatment was performed on the epidermal surface. Video was captured when the needles penetrated fully into the dermis. The video was then exported and filtered using MATLAB (The MathWorks Inc) software provided by FLIR, US to obtain a clean image of the heating phenomena produced by the RFMN system.

3 | RESULTS

3.1 | Evaluation of electrocoagulation

Histology of the porcine skin samples demonstrated coagulation thermal injury where the needle was inserted. In the histologic images (Figures 3A-E and 4A-J), the epidermis revealed the needle penetration site, demarcated by a focal region of darker purple stain, but did not show remarkable damage, if any, to the epidermis.

Area analysis of the thermal injury revealed a positive correlation for 1 MHz signal amplitude where increasing power resulted in a larger coagulation zone (Table 2). Histology results of the thermal injury induced by insulated needles (Figures 3A-E and 4A-E) demonstrated that 2 MHz resulted in a narrow and concentrated coagulation zone as compared to 1 MHz.

3.2 | Insulated microneedle 1 MHz vs noninsulated microneedle 2 MHz

Insulated needles are coated with a material such that 0.4 mm of the needle is uninsulated (Figure 1D).This allows energy to radiate from the uninsulated portion with much of the energy traveling down the insulated shaft to the needle tip. In contrast, a noninsulated needle (Figure 1D) allows for greater dispersion of energy throughout the length of the needle. Histology results demonstrated that using an insulated needle at 2 MHz can result in similar tissue coagulation histology when compared to a 1 MHz noninsulated needle (Figure 4A-J). When comparing 1 MHz insulated (Figure 3A-E) to 2 MHz insulated (Figure 4A-E) needles, the 1 MHz insulated needle resulted in ovular shaped tissue coagulation as compared to 2 MHz tissue coagulation that was columnar.

3.3 | Thermal diffusion evaluation of radiofrequency microneedling

Radiofrequency microneedling systems deliver energy to a specific skin layer producing an electrocoagulation shown previously in Figures 2 and 3. Figure 5 illustrates the heat diffusion when using an RFMN system under an infrared (IR) camera in an ideal system. Figure 6 shows a different result with the IR camera capturing a uniform block of radiofrequency energy dispersion. Additionally, Figure 6 suggests that even though the max RF conduction time on the system is 800 ms, the heating affect does not fully saturate until 10 seconds.

4 | DISCUSSION

There have been few published studies that examine the effects of RF electrocoagulation on epidermal and dermal tissue with most reports consisting of clinical observations. Proper selection of RFMN frequency, power, and needles is critical to procedure success.

For RFMN treatments, it is important to minimize epidermal thermal damage to decrease patient discomfort and downtime. In the current study, the RFMN device did not show any damage to the epidermis for 1 or 2 MHz insulated or noninsulated microneedles. 1 MHz produced larger coagulation areas than 2 MHz. This may be due to the greater wave period at 1 MHz compared to 2 MHz, allowing a higher voltage and current density gradient to move through the plated microneedles, enabling the electrocoagulation effect to radiate for a longer distance. The area of coagulation was less variable with higher power levels as demonstrated in the 2 MHz insulated needle coagulation areas in Table 2. These findings support previous study observations where coagulation was significantly

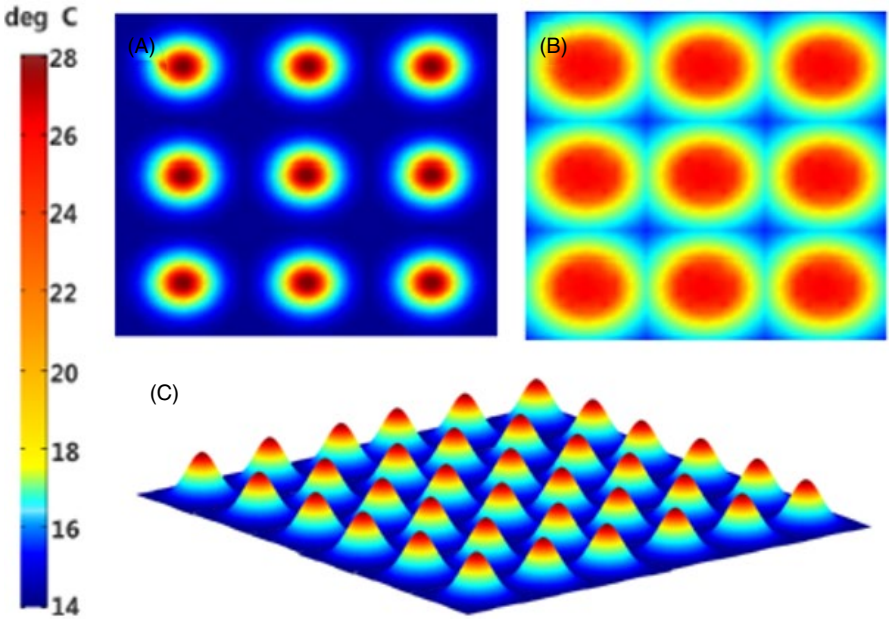

FIGURE 5 Representation of thermal temperature images under IR camera based off electrode placement of RFMN system. A, Representation after 800 ms RF conduction time. B, Representation after a few seconds of thermal dispersion. C, Representation of thermal zones for RFMN system

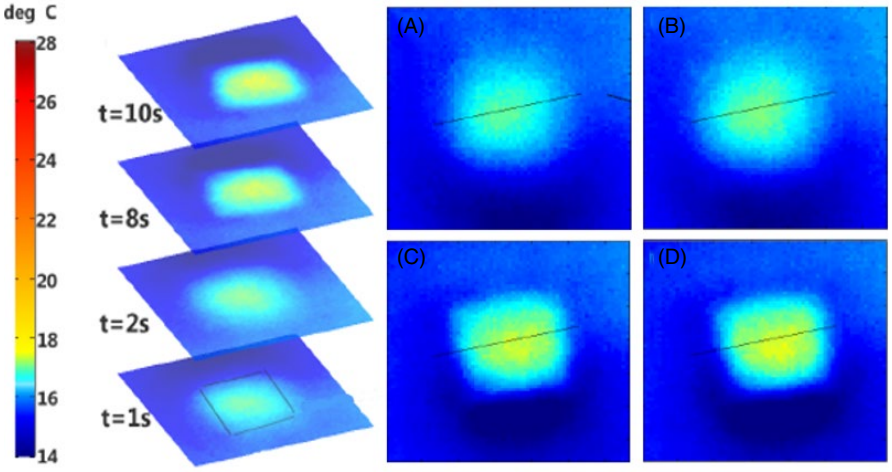

FIGURE 6 Thermal temperature images of application area using insulated microneedle electrodes at RF conduction time of 800 ms and at power level 10. A, 1 s, (B) 2 s, (C) 8 s, and (D) 10 s

affected with microneedle depth and RF conduction times.[8] Electrocoagulations also have variability due to bioimpedance or the resistance of the targeted tissue when using the RF modality.[9]

The reason why 1 MHz noninsulated and 2 MHz insulated needle electrocoagulation have similar histologic findings (Figure 4) may be due to frequency dispersion in the insulation material of the insulated needle.[10] This novel finding increases the utility of RF microneedling allowing the operator to switch between insulated and noninsulated needles with changing frequencies, giving the clinician more control over tissue coagulation without the need to switch needles. In this way, the insulated needle affords greater options for treatment compared to the noninsulated needle.

Heat transfer occurs when applying RFMN to a specific skin layer. At a high energy level, conduction occurs between the heated needle and the tissue, convection occurs between the heated needle and the blood and other fluids in the skin, and radiation occurs with radiofrequency dispersion where no transfer medium is needed. All three of these heat transfer methods result in block heating vs periodic, nonuniform heating that Figure 4 illustrated. Figure 4 assumes the heat only transferred through conduction between the needles and the tissue. The current study showed that heat transfer from the microneedles is more complex and disproved the assumption in Figure 4. Therefore, the study RFMN device produces uniform heat diffusion where the heat diffuses and fills the entire microneedle area (Figure 6) and not nonuniform heat diffusion where the heating does not fill the entire microneedle area (Figure 5).

Even though the study RFMN device produces block heating or uniform heating, the device still causes columnar or ovular electrocoagulation and not a uniform block of electrocoagulation. This may be due to conduction having the largest heat transfer effect rather than convection and radiation. It is important to consider convection and radiation when analyzing the RFMN effect on the skin. Convection and radiation may still play a key role in extracellular

matrix remodeling due to its heating effect seen in Figure 6. The block heating or uniform heating shown in Figure 6 demonstrates that the heat is confined within the area of the microneedle array and reduces safety concerns with radiofrequency devices.

Since full thermal diffusion occurs seconds after the set RF conduction time, it is important to be aware of possible bulk heating or bulk heat damage, which in turn would potentially cause epidermal damage and/or heat the subcutaneous layer. This bulk heat damage is undesirable due to less heated area control and potential patient adverse events.

Even though the porcine skin samples are not the same as human skin samples, it is the best substitute when needing large surface areas for biopsies. We believe that with knowledge now of radiofrequency diffusion effects through the use of RFMN can now help clinicians optimize settings for their patients and help guide further research in the RFMN space in the way of now optimizing clinical trials with the need of less biopsies due to the knowledge of these studies presented.

5 | CONCLUSION

The current study characterized the structural changes in porcine skin when bipolar radiofrequency was administered using insulated and noninsulated needles at 1 and 2 MHz. The findings suggest the 1 MHz insulated needle produces larger areas of electrocoagulation as the power level increases. A 2 MHz insulated needle induces similar histologic changes as a 1 MHz noninsulated needle. Finally, this research also demonstrated that radiofrequency heat dissipates seconds after the set conduction time requiring care when overlapping or stacking microneedle arrays to prevent bulk heating.

CONFLICT OF INTEREST

Shaun Wootten, BSE, and Lawrence Rheins, PhD, work for Aesthetics Biomedical, Inc Zoe Diana Draelos, MD, has served as a researcher and consultant for Aesthetics Biomedical, Inc.

DATA AVAILABILITY STATEMENT

The data that support the findings of this study are available from the corresponding author upon reasonable request.

ORCID

Shaun Wootten https://orcid.org/0000-0003-1768-4157
Zoe Diana Draelos https://orcid.org/0000-0001-9803-7415

REFERENCES

1. Cho SI, Chung BY, Choi MG, et al. Evaluation of the clinical efficacy of fractional radiofrequency microneedle treatment in acne scars and large facial pores. *Dermatol Surg*. 2012;38(7 Pt 1):1017-1024.
2. Peterson JD, Palm MD, Kiripolsky MG, et al. Evaluation of the effect of fractional laser with radiofrequency and fractionated radiofrequency on the improvement of acne scars. *Dermatol Surg*. 2011;37(9):1260-1267.
3. Man J, Goldberg DJ. Safety and efficacy of fractional bipolar radiofrequency treatment in Fitzpatrick skin types V-VI. *J Cosmet Laser Ther*. 2012;87(6):179-183.
4. Lee SJ, Goo JW, Shin J, et al. Use of fractionated microneedle radiofrequency for the treatment of inflammatory acne vulgaris in 18 Korean patients. *Dermatol Surg*. 2012;38(3):400-405.
5. Van NB, Alster TS. Laser treatment of dark skin: a review and update. *J Drugs Dermatol*. 2009;8(9):821-827.
6. Taheri A, Mansoori P, Sandoval LF, et al. Electrosurgery: part II. Technology, applications, and safety of electrosurgical devices. *J Am Acad Dermatol*. 2014;70(4):607-e1.
7. Brill AI. Bipolar electrosurgery: convention and innovation. *Clin Obstet Gynecol*. 2008;51(1):153-158.
8. Zheng Z, Goo B, Kim DY, et al. Histometric analysis of skin-radiofrequency interaction using a fractionated microneedle delivery system. *Dermatol Surg*. 2014;40(2):134-141.
9. Taheri A, Mansoori P, Sandoval LF, et al. Electrosurgery: part I. Basics and principles. *J Am Acad Dermatol*. 2014;70(4):591-e1.
10. Tao J, Zhao CZ, Zhao C, et al. Extrinsic and intrinsic frequency dispersion of high-k materials in capacitance-voltage measurements. *Materials*. 2012;5(12):1005-1032.

How to cite this article: Wootten S, Zawacki ZE, Rheins L, Meschter C, Draelos ZD. An evaluation of electrocoagulation and thermal diffusion following radiofrequency microneedling using an in vivo porcine skin model. *J Cosmet Dermatol*. 2020;00:1–7. https://doi.org/10.1111/jocd.13690